JCI The Journal of Clinical Investigation

Collecting duct–specific gene inactivation of αENaC in the mouse kidney does not impair sodium and potassium balance

Isabelle Rubera, … , Edith Hummler, Bernard C. Rossier

J Clin Invest. 2003;112(4):554-565. https://doi.org/10.1172/JCI16956.

Article Nephrology

Aldosterone controls the final sodium reabsorption and potassium secretion in the kidney by regulating the activity of the epithelial sodium channel (ENaC) in the aldosterone-sensitive distal nephron (ASDN). ASDN consists of the last portion of the distal convoluted tubule (late DCT), the connecting tubule (CNT), and the collecting duct (CD) (i.e., the cortical CD [CCD] and the medullary CD [MCD]). It has been proposed that the control of sodium transport in the CCD is essential for achieving sodium and potassium balance. We have tested this hypothesis by inactivating the α subunit of ENaC in the CD but leaving ENaC expression in the late DCT and CNT intact. Under salt restriction or under aldosterone infusion, whole-cell voltage clamp of principal cells of CCD showed no detectable ENaC activity, whereas large amiloride-sensitive currents were observed in control littermates. The animals survive well and are able to maintain sodium and potassium balance, even when challenged by salt restriction, water deprivation, or potassium loading. We conclude that the expression of ENaC in the CD is not a prerequisite for achieving sodium and potassium balance in mice. This stresses the importance of more proximal nephron segments (late DCT/CNT) to achieve sodium and potassium balance.

Collecting duct–specific gene inactivation of αENaC in the mouse kidney does not impair sodium and potassium balance

Isabelle Rubera,[1] Johannes Loffing,[2] Lawrence G. Palmer,[3] Gustavo Frindt,[3] Nicole Fowler-Jaeger,[1] Daniel Sauter,[2] Tom Carroll,[4] Andrew McMahon,[4] Edith Hummler,[1] and Bernard C. Rossier[1]

[1]Institut de Pharmacologie et de Toxicologie, Université de Lausanne, Lausanne, Switzerland
[2]Institute of Anatomy, University of Zurich, Zurich, Switzerland
[3]Department of Physiology and Biophysics, Weill Medical College of Cornell University, New York, New York, USA
[4]Harvard University, Department of Molecular and Cellular Biology, Cambridge, Massachusetts, USA

Aldosterone controls the final sodium reabsorption and potassium secretion in the kidney by regulating the activity of the epithelial sodium channel (ENaC) in the aldosterone-sensitive distal nephron (ASDN). ASDN consists of the last portion of the distal convoluted tubule (late DCT), the connecting tubule (CNT), and the collecting duct (CD) (i.e., the cortical CD [CCD] and the medullary CD [MCD]). It has been proposed that the control of sodium transport in the CCD is essential for achieving sodium and potassium balance. We have tested this hypothesis by inactivating the α subunit of ENaC in the CD but leaving ENaC expression in the late DCT and CNT intact. Under salt restriction or under aldosterone infusion, whole-cell voltage clamp of principal cells of CCD showed no detectable ENaC activity, whereas large amiloride-sensitive currents were observed in control littermates. The animals survive well and are able to maintain sodium and potassium balance, even when challenged by salt restriction, water deprivation, or potassium loading. We conclude that the expression of ENaC in the CD is not a prerequisite for achieving sodium and potassium balance in mice. This stresses the importance of more proximal nephron segments (late DCT/CNT) to achieve sodium and potassium balance.

J. Clin. Invest. **112**:554–565 (2003). doi:10.1172/JCI200316956.

Introduction

The most important functions of aldosterone are to promote sodium reabsorption and potassium secretion across epithelia that display an electrogenic sodium transport (1) mediated by the amiloride-sensitive epithelial sodium channel (ENaC). ENaC is a heteromultimeric protein made of three subunits, termed α, β, and γ (2). When all three subunits are expressed in the same cell (for instance, the *Xenopus* oocyte), a preferential assembly into a heteromeric structure is observed (3, 4). Binding experiments demonstrated a close correlation between the number of channel molecules present at the cell surface and the current expressed in individual oocytes. Complexes comprising α, αβ, αγ, and βγ subunits reached the cell surface, though less efficiently than did αβγ-injected oocytes. No signal could be detected on oocytes injected with either β or γ subunits alone. The α subunit thus plays an essential chaperone role in the trafficking of the channel to the cell surface (5), as well as forming part of the pore. Coexpression of the three subunits, however, leads to maximal ENaC activity at the cell surface. The importance of each subunit in preferential assembly in vivo is underscored by gene inactivation of α, β, or γ subunits of ENaC in the mouse (6). A striking feature of inactivation of either subunit was 100% lethality within 2–4 days after birth. The critical importance of ENaC-mediated sodium transport in vivo has also been emphasized by the description of two human monogenic diseases that have been linked to ENaC subunit genes. Gain-of-function mutations in the β or γ subunit of ENaC lead to a hypertensive phenotype (Liddle syndrome), a paradigm for salt-sensitive hypertension (7). Loss-of-function mutations in the α, β, or γ subunit genes of

Received for publication September 20, 2002, and accepted in revised form June 10, 2003.

Address correspondence to: Bernard C. Rossier, Institut de Pharmacologie et de Toxicologie, Rue du Bugnon 27, CH-1005 Lausanne, Switzerland.
Phone: 41-21-692-5351; Fax: 41-21-692-5355;
E-mail: bernard.rossier@ipharm.unil.ch.
Isabelle Rubera, Johannes Loffing, and Edith Hummler contributed equally to this work.

Conflict of interest: The authors have declared that no conflict of interest exists.

Nonstandard abbreviations used: epithelial sodium channel (ENaC); aldosterone-sensitive distal nephron (ASDN); distal convoluted tubule (DCT); connecting tubule (CNT); collecting duct (CD); cortical CD (CCD); medullary CD (MCD); outer MCD (OMCD); inner MCD (IMCD); adrenalectomized (adx); glomerular filtration rate (GFR); pseudohypoaldosteronism type 1 (PHA-1); X-galactosidase (X-gal); aquaporin-2 (AQP2); sodium/calcium exchanger (NCX); calbindin D28K (CB); sodium thiazide–sensitive chloride cotransporter (NCC).

ENaC cause pseudohypoaldosteronism type 1, an autosomal recessive form of a severe salt-losing syndrome with hyperkalemia and metabolic acidosis (8).

In the kidney, aldosterone-dependent regulation of ENaC takes place in the aldosterone-sensitive distal nephron (ASDN), which was defined (9) as comprising the end of the distal convoluted tubule (late DCT), the connecting tubule (CNT), and the collecting duct (CD). The latter includes the cortical CD (CCD) and the outer and inner medullary CD (OMCD and IMCD, respectively). In the CNT, CCD, and OMCD, the electrogenic sodium transport provides the main electrochemical gradient for the secretion of potassium across ROMK, a potassium channel coexpressed with ENaC in the apical membrane of CNT cells and of CCD and OMCD principal cells. Inhibition of ENaC in vivo leads to hyperkalemia and metabolic acidosis, whereas activation of ENaC will lead to the opposite effect — that is, hypokalemia and metabolic alkalosis. Salt intake is one of the primary physiological stimuli controlling aldosterone secretion by the adrenals. In rats on a normal- or high-salt diet, plasma concentrations of aldosterone are low, and ENaC activity measured by patch clamp of the apical membrane of CCD principal cells is not detectable. On a sodium-deficient diet, plasma aldosterone levels rise rapidly and ENaC activity increases dramatically (10). Specific antibodies have been raised against each subunit (11, 12), allowing the study of ENaC regulation in mouse and rat ASDNs in vivo (12, 13). On a high-salt diet (low plasma aldosterone), ENaC subunits are undetectable on the apical membrane of cells lining the entire ASDN, which is consistent with the electrophysiological data discussed above. α subunit was not detected, whereas β and γ subunits were localized in a cytoplasmic pool that has yet to be precisely identified (13). The predominant intracellular localization of the ENaC channel complex is consistent with the electrophysiological data in rats (10). On a low-salt diet, which increased plasma aldosterone by twofold, all three ENaC subunits were observed in the subapical cytoplasm and the apical membrane of late DCT and CNT and, less prominently, in CCD cells (13). Apical immunostaining progressively decreased along CCDs with a concomitant increased cytoplasmic staining for β and γ subunits. These findings are consistent with electrophysiological data obtained in the rat model (10). The data in vivo are also consistent with the preferential ENaC assembly model derived from the *Xenopus* expression model discussed above (4). Recently, we have shown that injection of aldosterone in adrenalectomized (adx) rats induces αENaC subunit expression along the entire ASDN within 2 hours, whereas βENaC and γENaC are constitutively expressed in an intracellular cytoplasmic pool (9). In the proximal ASDN (late DCT and CNT only), ENaC is shifted toward the apical cellular pole and the apical plasma membrane within 2 and 4 hours, respectively. In the same adx rat model, it has been shown previously that low concentrations of aldosterone (in the presence of dexamethasone to prevent any change in the glomerular filtration rate [GFR]) were able to induce a large effect on sodium and potassium excretion within 3 hours (14). Altogether, these physiological and immunolocalization observations emphasize the importance of understanding the respective roles of aldosterone target cells in the late DCT/CNT nephron segment versus the collecting duct. One could postulate that the early effect of aldosterone on ENaC to achieve sodium balance could take place only in late DCT and CNT, whereas the long term effect of aldosterone to achieve sodium balance under a prolonged and severe salt restriction will take place along the ASDN, including the entire collecting duct.

The aim of the present study was to examine the consequence of inactivating ENaC α subunit in CDs. Classical gene inactivation of the α, β, or γ subunit leads to a perinatal-lethal phenotype, characterized by lung fluid–clearance failure (15) and/or by an acute pseudohypoaldosteronism type 1 (PHA-1) with severe hyperkalemia and metabolic acidosis (16, 17). Obviously, these models cannot help in addressing the question raised, since ENaC activity is deleted in the entire nephron and the PHA phenotype cannot be studied in the adult animal because complete gene inactivation of any of the three *Scnn1* genes (encoding for αENaC, βENaC, and γENaC) leads to early postnatal death. We generated a conditional allele at the gene locus encoding the α subunit (*Scnn1a*) (18) and, using a *Cre* mouse under a *Hoxb7* promoter, we were able to inactivate αENaC along the entire collecting duct.

Methods

Animals. Three subunits (α, β, and γENaC) have been characterized, encoded by various genes on human chromosomes 12 (*SCNN1A*) and 16 (*SCNN1C*, *SCNN1B*). In the mouse, the genes have been localized on chromosomes 6 (*Scnn1a*) and 7 (*Scnn1b, Scnn1c*) (19, 20). The generation of $Scnn1a^{lox}$ conditional knockout mice has been described previously (18). Briefly, using ES technology, we obtained a loxed *Scnn1a* allele. We showed that the position of the remaining *loxP* sites did not interfere with the transcription of the *Scnn1a* locus. Resulting $Scnn1a^{loxlox}$ mice did not show any reduction of αENaC mRNA levels as compared with wild-type littermates. Male mice carrying the $Scnn1a^{lox}$ allele were bred to an *EIIa-Cre* deleter strain to constitutively remove exon 1 in vivo. The resulting *Scnn1a* allele was named $Scnn1a^{tm2}$ to distinguish from the $Scnn1a^{tm1}$ allele we had generated earlier (15). As expected, interbreeding of $Scnn1a^{tm2/+}$ mutant mice resulted in the absence of any living $Scnn1a^{tm2/tm2}$ homozygous mutant mice 4 days after birth. We therefore concluded that (a) exon 1 can be efficiently removed by *Cre* recombinase in vivo, and (b) complete absence of exon 1 leads to a lethal phenotype, as described for αENaC deficiency of the $Scnn1a^{tm1}$ allele.

Homozygous $Scnn1a^{loxlox}$ mice (18) were bred with a transgenic line expressing recombinase *Cre* under the *Hoxb7* promoter (21). The resulting offspring

were genotyped by PCR on genomic tail DNA (18). The presence of the *Cre* transgene was detected by PCR, using the primers 5′-CCTGGAAAATGCTTCTGTCCG-3′ and 5′-CAGGGTGTTATAAGCAATCCC-3′ to amplify a 350-bp fragment (36 cycles of 1 minute at 94°C, 1 minute at 56°C, and 1 minute at 72°C). Interbreeding *Scnn1a*^{loxlox} mice with *Scnn1a*^{loxloxCre} mice generates 50% *Scnn1a*^{loxlox} (control) and 50% *Scnn1a*^{loxloxCre} (experimental) mice.

In order to characterize the activity of the *Hoxb7:Cre* transgene in the P1 collecting duct system, mice doubly transgenic for *Hoxb7:Cre* and the *Rosa 26* reporter allele were crossed to Swiss Webster female mice. For whole-mount observation, the entire intact urogenital system was removed from euthanized P1 pups and stained with X-galactosidase (X-gal) (21). Because of poor penetration of the staining solution in intact kidneys, a modified procedure was used for observing expression deeper than the outer cortex. In order to observe more internal structures, kidneys were sliced after fixation into thick (approximately 2-mm) sections with a razor blade and then stained with X-gal. Individual thick sections were embedded in 15% gelatin in PBS and sectioned on a vibratome. Twenty-five–micrometer sections were mounted in glycerol, coverslipped, and photographed using a Nikon stereoscope (Figure 1, a and b) or a Leica compound microscope (Figure 1c).

Body weight. *Scnn1a*^{loxlox} and *Scnn1a*^{loxloxCre} littermate mice (10–14 weeks old) fed with a regular diet (0.23% sodium) were weighed at day 0 to determine the reference weight. Then, mice were fed a sodium-deficient diet (0% sodium) with free access to tap water, and their weights were monitored at the same time of day for 7 consecutive days.

Sodium-restriction diet and water deprivation. Protocols involving animals were reviewed and approved by the State Authority (Commission du Service Veterinaire Cantonal, Lausanne, Switzerland). Mice (20–24 weeks old) were fed with a normal-salt diet (0.23% sodium, 0.95% potassium; regular-salt diet from Provimi Kliba Nafag, Rotterdam, The Netherlands) followed by 6 days with a sodium-deficient diet (ICN Biomedical, Costa Mesa, California, USA; protocol A) or 5 days with a sodium-deficient diet, followed by 23 hours of water deprivation (protocol B). Blood and urine samples were collected before and after 23 hours of water deprivation. Some animals ("Aldo-salt," protocol C) were infused with aldosterone under standard-salt diet through subcutaneous osmotic minipumps (Alzet model 1002; Alza Corp., Palo Alto, California, USA) (22) for 6 days. Aldosterone was dissolved in polyethylene glycol-300 at concentration of 2 mg/ml. The infusion rate was 10 μg per day.

Potassium loading. In another set of experiments (protocol D), animals (20–24 weeks old) were fed for 48 hours with a high-potassium diet containing 2.6% potassium followed by 48 hours with a diet containing 6% potassium with free access to drinking water. High-potassium diets were prepared by adding KCl to gelatin mixed with food to obtain a final concentration of 2.6% or 6% potassium.

Urine and serum analysis. Urine samples were collected by spontaneous voiding. Urine sodium and potassium were measured and normalized to creatinine concentrations (millimoles of sodium per milligram of creatinine). For urine samples collected after 5 days of salt restriction, ion concentrations were determined with an ion chromatography system (DX 600, Dionex Corp., Sunnyvale, California, USA). Urine osmolality was measured with a vapor pressure osmometer (Wescor Inc., Logan, Utah, USA) and expressed as milliosmoles per kilogram of H_2O. Blood samples were collected from the retro-orbital venous plexus under anesthesia. Plasma creatinine and sodium/potassium concentrations were measured, using a Kodak Ektachem analyzer (Johnson and Johnson Ortho-Clinical Diagnostics, New Brunswick, New Jersey, USA). Aldosterone assays were measured in duplicate on plasma samples using a [^{125}I]RIA (detection limit, 6 pg/ml).

Immunohistochemistry. For the present study, we generated a second generation of antibodies against α, β, and γ subunits, using the same GST fusion proteins as previously described (11). Five *Scnn1a*^{loxlox} and 5

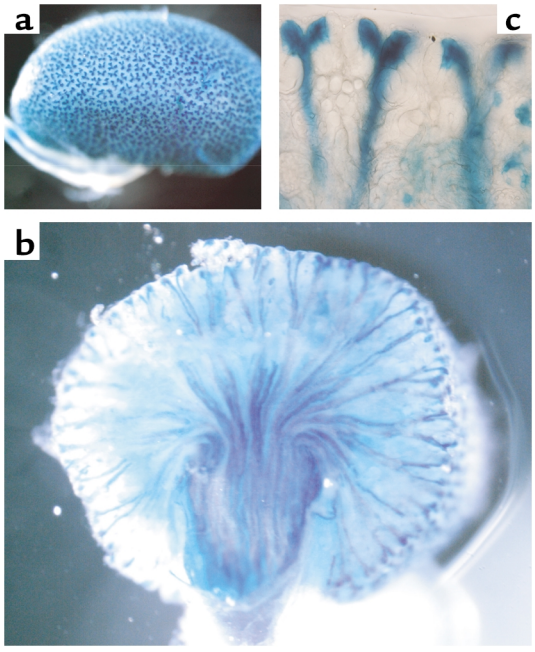

Figure 1
Expression of the *Hoxb7* promoter using the *CreRosa 26* reporter system. The activity of *Hoxb7-Cre* is assayed by analysis of the Rosa reporter. (**a**) An intact P1 kidney stained with X-gal showing that *Hoxb7-Cre* is active in the CCDs and ureter (magnification, ×20). (**b**) A stained, thick section reveals *Hoxb7-Cre* activity throughout the CCD and MCD system (magnification, ×50). (**c**) 20 μM sections of stained kidneys demonstrate that *Hoxb7-Cre* is active in most if not all cells of the CD system (magnification, ×400). Some additional, mosaic staining is viewed in cells of the CNT and/or DCT, most likely due to mixing of cells at the fusion point of these two lineages.

Scnn1a^{loxloxCre} mice were kept for 7 days on a sodium-deficient diet (0% sodium). Kidneys of these mice were fixed by intravascular perfusion and processed for immunohistochemistry according to previously described procedures (9). Serial cryosections (4- to 5-μm thick) were incubated with rabbit antisera against rat αENaC (dilution, 1:1,000), rat βENaC (dilution, 1:2,000), or γENaC (dilution, 1:500). For some experiments, we also used an affinity-purified rabbit anti-rat aquaporin-2 (AQP2) antibody (Alamone Labs, Jerusalem, Israel), affinity-purified rabbit anti-canine sodium/calcium exchanger (NCX) (Swant, Bellinzona, Switzerland), and monoclonal mouse anti-chicken calbindin D28K (CB; Sigma-Aldrich, St Louis, Missouri, USA) diluted 1:1,000, 1:1,000, and 1:20,000, respectively. Incubations with the primary antibodies, diluted in PBS/1% BSA, took place overnight at 4°C. After repeated rinsing with PBS, binding sites of the primary antibodies were revealed with Cy3-conjugated donkey anti-rabbit IgG and FITC-conjugated goat anti-mouse IgG (both from Jackson ImmunoResearch Laboratories, West Grove, Pennsylvania, USA), diluted 1:1,000 and 1:40, respectively. Finally, sections were washed with PBS and mounted with DAKO-Glycergel containing 2.5% DABCO (Sigma-Aldrich) to retard fading. For control of unspecific binding of anti-ENaC antibodies, we performed control experiments in which the anti-α, anti-β, and anti-γ ENaC antisera were preincubated with the respective immunogenic GST fusion protein (final concentration of the GST fusion protein, 0.2 mg/ml). Sections were studied by epifluorescence with a Polyvar microscope (Reichert Jung, Vienna, Austria). Digital images were acquired with a charge-coupled-device camera (Visicam 1280, Visitron Systems, Puching, Germany) and processed by Image-Pro and Photoshop software. The cortical ASDN segments were identified according to well-defined morphological and immunohistochemical criteria. In brief, the late DCT and the CNT, both located in the cortical labyrinth, are characterized by high expression of CB and NCX, which is slightly stronger in DCT than in CNT. The CCD, localized in the medullary ray, is characterized by weak CB and no significant NCX expression.

Electrophysiology. Whole-cell currents were measured on CCDs, as described previously (4, 22). After sacrificing the animals (protocol A or C), the kidneys were removed, and CCDs were dissected free and opened manually to expose the luminal surface. The split tubules were attached to a small plastic rectangle coated with Cell-Tak (Collaborative Research, Bedford, Massachusetts, USA) and placed in a perfusion chamber mounted on an inverted microscope. The chamber was continuously perfused with solution consisting of (in mM) 135 sodium methane sulfonate, 5 KCl, 2 $CaCl_2$, 1 $MgCl_2$, 2 glucose, 5 $BaCl_2$, and 10 HEPES adjusted to pH 7.4 with NaOH, prewarmed at 37°C. The patch-clamp pipettes were filled with solutions containing (in mM) 7 KCl, 123 aspartic acid, 20 CsOH, 20 TEAOH, 5 EGTA, 10 HEPES, 3 MgATP, and 0.3 NaGDPβS adjusted to pH 7.4 with KOH. The major salt in this solution was potassium aspartate. Whole-cell currents were recorded in the absence and the presence of 10 μM amiloride.

Statistical analysis. Results are given as means ± SE. Statistical significance was assessed by using an unpaired *t* test. A *P* value of less than 0.05 was considered significant.

Results

Inactivation of α ENaC in the collecting duct. The *Scnn1a*^{lox} conditional knockout mice (strain 129B6F$_1$) were used for analyzing ENaC deficiency in adult kidney by cross-breeding to *Hoxb7:Cre*–expressing mouse lines. *Hoxb7* is a member of the homeobox gene family, which has been proposed to regulate cell fate decisions during metanephros development and, more specifically, between ureteric bud branching and the final maturation of the CD (21, 23–27). In order to verify the

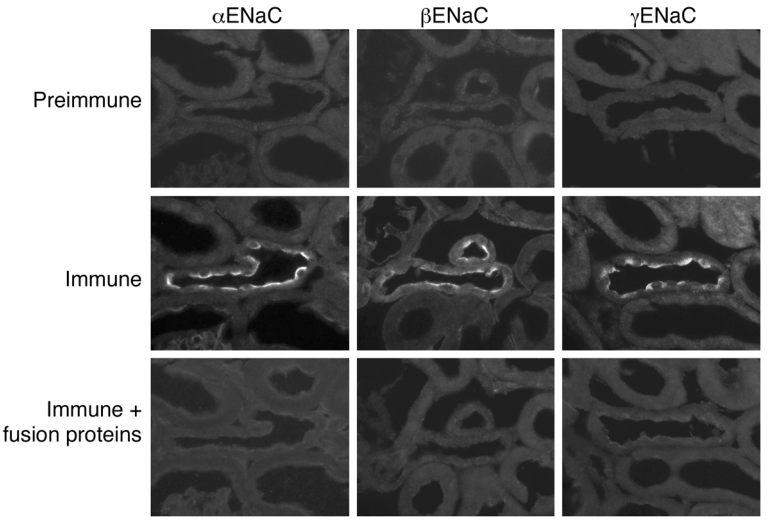

Figure 2
Immunohistochemical characterization of ENaC antibodies on cryosections of kidneys from *Scnn1a*$^{lox/lox}$ mice kept on a sodium-free diet for 7 days. Immune sera for α, β, and γENaC show a bright apical immunostaining in CNT profiles that is not seen on sections incubated with preimmune sera or with immune sera in the presence of the immunogenic fusion proteins. Each column of images represents immunofluorescence on consecutive cryosections.

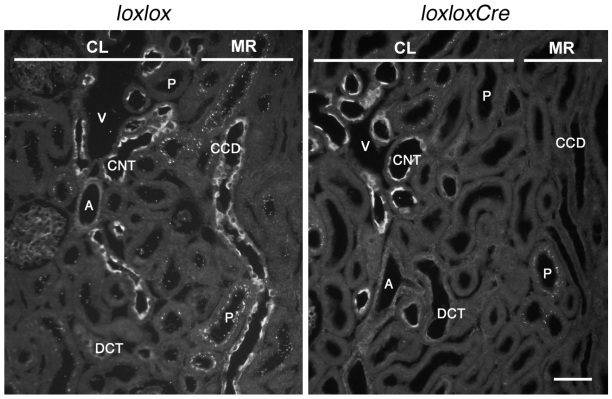

Figure 3
Immunofluorescent detection of αENaC in kidney cortex of *Scnn1a*^{loxlox} and *Scnn1a*^{loxloxCre} mice kept on a sodium-free diet for 6 days. In mice of both genotypes, αENaC is highly abundant in CNT profiles grouped around cortical radial arteries and veins located in the cortical labyrinth. Late DCT profiles exhibit a weak immunostaining. CDs running in the medullary rays are stained in *loxlox* (control) mice but are unstained in *loxloxCre* (experimental) mice. A, arteries; V, veins; CL, cortical labyrinth; MR, medullary rays; P, proximal tubules. Scale bar, 50 μm.

organ/tissue specificity of *Hoxb7* promoter expression in CDs, *Hoxb7:Cre* mice were bred to a *CreRosa 26* strain (28). As shown in Figure 1, a kidney from a 1-day-old mouse showed a typical staining of the CD as seen at the surface of the kidney (Figure 1a) or on its whole section (Figure 1b), whereas 20-μm sections (Figure 1c) showed homogeneous staining of the entire CD. There was no evidence of mosaicism at this resolution. Lung, colon, skin, liver, heart, and brain were negative (data not shown). According to these data, the *Hoxb7:Cre* mice should be able to specifically inactivate αENaC along the entire CD. Since the α subunit synthesis and its assembly with the β and γ subunits is limiting in the export of ENaC active channels to the apical membrane, gene inactivation of αENaC should lead to a loss of function of ENaC in the apical membrane, with β and γ subunits remaining in an intracellular compartment.

CD gene inactivation of αENaC prevents the apical localization of β and γ subunits in CD but not in late DCT and CNT cells. As shown in Figure 2, the immune sera against α, β, and γ subunits, respectively, showed a bright apical staining in CNT from control (*loxlox*) mice on a sodium-deficient diet, whereas sections stained with preimmune serum or immune serum preincubated with GST fusion proteins remained unstained. On a regular diet, as previously described (13), α staining was barely detectable, whereas β and γ subunits were restricted to an intracellular cytoplasmic compartment (data not shown). Immunofluorescent detection of αENaC in kidney cortex of *Scnn1a*^{loxlox} and *Scnn1a*^{loxloxCre} mice is shown in Figure 3. In mice of both genotypes, αENaC is highly abundant in CNT profiles grouped around the cortical radial vessels in the cortical labyrinth. Late DCT profiles exhibit a weak immunostaining. CDs running in the medullary rays are stained in *Scnn1a*^{loxlox} mice but are unstained in *Scnn1*^{loxloxCre} mice. In the *Scnn1a*^{loxloxCre} mice on a sodium-deficient diet (Figure 4a, left), bright apical immunostaining was seen along the CNT cell, but the staining abruptly stopped at the junction with the CCD (arrows). To ensure that the CNT/CD junction was the site of this abrupt staining transition, consecutive sections were stained with antibodies against AQP2, a water channel known to be expressed across the CNT/CD junction (Figure 4a, right). As shown in Figure 4b, immunofluorescent

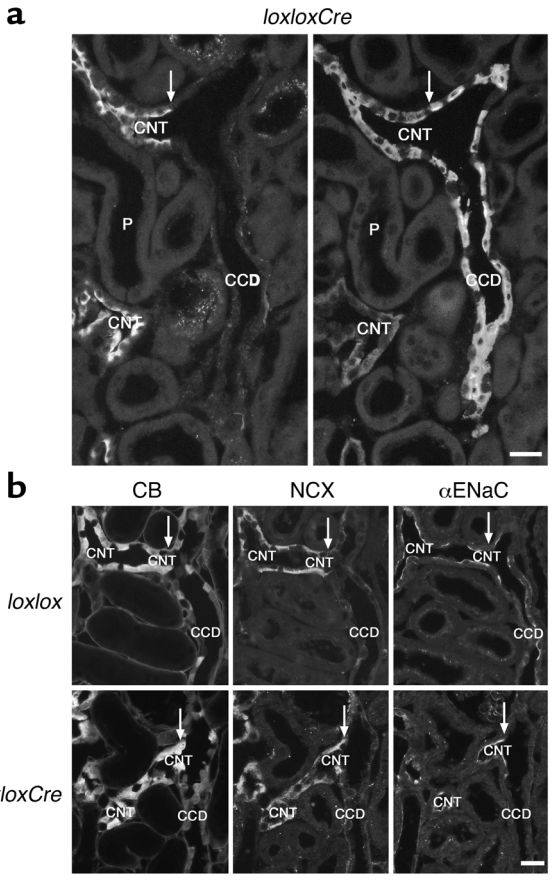

Figure 4
Transition of CNT to CCD in the kidney of *Scnn1a*^{loxloxCre} and *Scnn1a*^{loxlox} mice kept on a sodium-free diet for 6 days. (**a**) Immunofluorescence on consecutive cryosections with rabbit antibodies against αENaC and AQP2. Bright apical αENaC immunofluorescence ceases abruptly at the transition from CNT to CCD (arrows). AQP2 is seen in CNT and CCD. AQP2-negative cells in CNT and CCD are intercalated cells; the weak, punctuate staining in some tubular cells was not localized at the apical membrane, was occasionally observed with the αENaC antibody, and is nonspecific. P, proximal tubule. Scale bar, ~20 μm. (**b**) Immunofluorescent detection of CB, NCX, and αENaC on consecutive cryosections from kidneys of *loxlox* (control) and *loxloxCre* (experimental) mice. In mice of both genotypes, the sharp transition from CNT to CCD (arrows) is characterized by a drop of cytoplasmic CB immunostaining and a breakoff, i.e., discontinuity, of basolateral NCX abundance. In the *Scnn1a*^{loxlox} mouse, apical αENaC immunostaining continues from the CNT to the CCD, whereas in *Scnn1a*^{loxlox} mice, αENaC immunoreactivity is seen in CNT but not CCD. Scale bar, 20 μm.

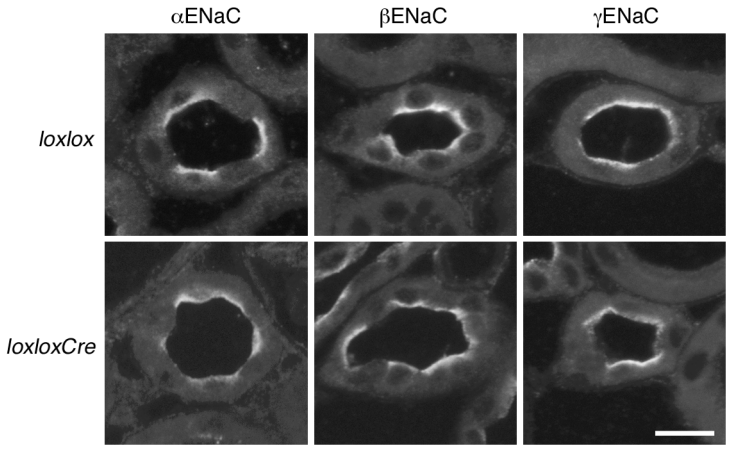

Figure 5
CNT profiles of kidneys from *Scnn1a*^{loxlox} and *Scnn1a*^{loxloxCre} mice kept on a sodium-free diet for 6 days. Immunofluorescence on cryosections with rabbit antibodies against α, β, and γENaC is shown. In mice of both genotypes, a bright apical immunostaining for α, β, and γENaC is seen in CNT cells. Unstained cells in the CNT profiles are intercalated cells. Scale bar, 15 μm.

detection of CB (left), NCX (middle), and αENaC (right) on consecutive cryosections from kidneys of *Scnn1a*^{loxlox} and *Scnn1a*^{loxloxCre} mice confirms the proper identification of the CNT/CCD junction.

Since the α subunit is normally expressed in CNTs of the experimental group, the expectation is that β and γ subunits should be colocalized with α in CNTs, as in control animals. By contrast, β and γ should stay in the cytoplasmic compartment in CCDs of *Scnn1a*^{loxloxCre} mice but should be translocated to the apical membrane of control animals on the same sodium-deficient diet. These expectations were supported by the immunofluorescent data in CNTs (Figure 5) and in CCDs (Figure 6). In *Scnn1a*^{loxlox} mice, immunostaining for α, β and γENaC was seen at the luminal membrane along the late DCT, CNT, CCD, and OMCD. Apical immunostaining was bright in CNTs (Figure 5) and progressively decreased along the CCD (Figure 6) before it almost completely vanished in OMCDs of the inner stripe (Figure 7). These results are consistent with our previous findings on an axial gradient along the ASDN of apically localized ENaC in wild-type mice on dietary sodium restriction. In *Scnn1a*^{loxloxCre} mice, apical localization of all three ENaC subunits was seen only in late DCT (not shown) and CNT (Figure 5). In CCD (Figure 6) and OMCD (Figure 7), αENaC was undetectable, and β and γENaC were found exclusively in intracellular compartments diffusely distributed throughout the cytoplasm of CCD and OMCD cells. To exclude any significant mosaicism, we determined by immunofluorescence in the *loxloxCre* mice the percentage of αENaC-positive cells in the CCD and OMCD (1.46 ± 0.32% and 0.07 ± 0.04%, respectively [mean ± SEM]; n = 5 mice; more than 500 cells per mouse and segment were analyzed). Thus, *Hoxb7*-mediated recombination was highly effective. In IMCDs from mice of both genotypes, ENaC subunits were undetectable by immunofluorescence (data not shown).

Gene inactivation of αENaC in CDs leads to a complete loss of ENaC channel activity in the apical membrane of CCD principal cells. To test whether the absence of an immunodetectable pool of ENaC subunits at the apical membrane of *Scnn1a*^{loxloxCre} homozygous mutant

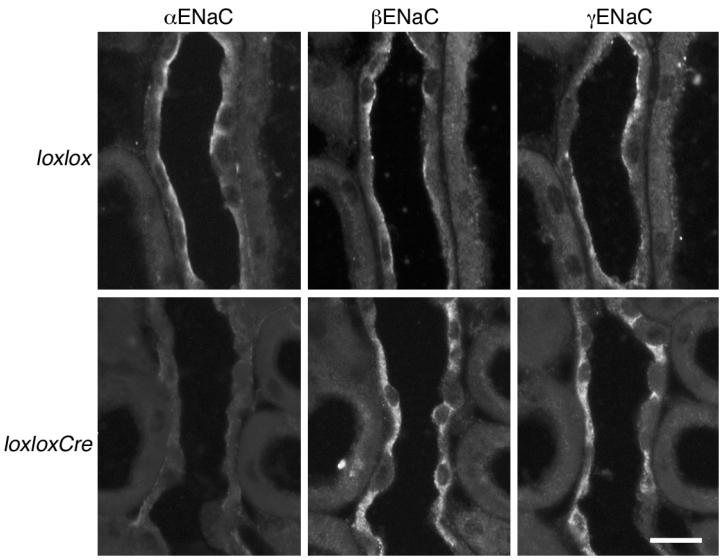

Figure 6
CCD profiles of kidneys from *Scnn1a*^{loxlox} and *Scnn1a*$^{loxlox-Cre}$ mice kept on a sodium-free diet for 6 days. Immunofluorescence on consecutive cryosections with rabbit antibodies against α, β, and γENaC. CCD cells of an *Scnn1a*^{loxlox} mouse show a weak but distinct apical immunostaining for α, β, and γENaC. Note the absence of αENaC immunostaining and the diffuse granular cytoplasmic localization of β and γENaC immunostaining in CCD cells of the *Scnn1a*^{loxloxCre} mouse. Unstained cells in the CCD profiles are intercalated cells. Scale bar, 20 μm.

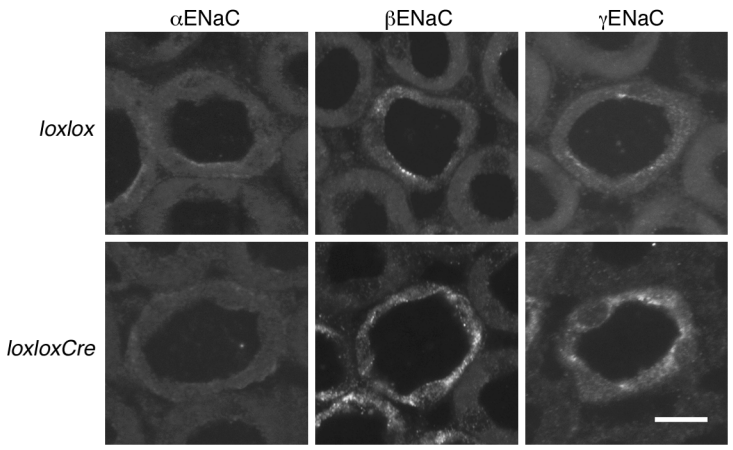

Figure 7
OMCD profiles of kidneys from *Scnn1a*^{loxlox} and *Scnn1a*^{loxloxCre} mice kept on a sodium-free diet for 6 days. Immunofluorescence on cryosections with rabbit antibodies against α, β, and γENaC. Some OMCD cells of *Scnn1a*^{loxlox} mice show a very faint apical immunostaining for α, β, and γENaC. OMCD cells of *Scnn1a*^{loxloxCre} mice lack αENaC immunostaining and show a diffuse cytoplasmic localization of β and γENaC immunostaining. Scale bar, 15 μm.

mice corresponded to the disappearance of active channels at the plasma membrane, CCDs were dissected from control and mutant mice after 6 days of salt restriction. Before salt restriction (day 0) (Table 1), plasma aldosterone levels of control and experimental mice were similar. Plasma levels were even lower in the experimental group, showing no evidence for a salt-losing syndrome and hypovolemia. After 5 days of salt restriction (day 5), plasma aldosterone levels of control and experimental groups increased significantly above day 0 values (8-fold and 11-fold [$P < 0.01$], respectively), but there was no significant difference between the two groups ($P < 0.6$). The tubules were split open, as described for the rat model (29), and sodium channel activity was assessed as the whole-cell amiloride-sensitive current. Typical current-voltage relationships (Figure 8) in the presence and absence of amiloride (10 μM) were recorded. In *Scnn1a*^{loxlox} mice, the amiloride-sensitive current (I_{Na}) was 102 ± 25 pA per cell (Table 2, top). In *Scnn1a*^{loxloxCre} mice, amiloride-sensitive current was undetectable under the same experimental condition. The difference between control and experimental animals was significant ($P < 0.001$). Thus, despite a strong hormonal stimulus to activate ENaC, the *Scnn1a*^{loxloxCre} mice remained totally unresponsive, which is consistent with the lack of an immunodetectable pool of α, β, or γ subunits at the apical membrane of the mutant cell. Maximal sodium reabsorption in the CCD requires both elevated mineralocorticoid and significant sodium delivery to the CCD, as would occur in deoxycorticosterone-treated rats on a normal-sodium diet. Low sodium delivery to the CCD may downregulate sodium transporters regardless of high mineralocorticoid levels (30). This raises the question of whether the presence or absence of ENaC activity (as measured here by patch clamp) in the CCDs of salt-depleted *Scnn1a*^{loxlox} versus *Scnn1a*^{loxloxCre} mice may reflect, in part, changes in sodium delivery to the CCD. To address this question, we performed a second series of experiments in aldosterone-treated mice on a standard-sodium diet (Table 2, bottom). In these animals, sodium delivery to the CCD is elevated (by mineralocorticoid escape), and aldosterone levels are high. Under these circumstances, we maximize the chance to detect a significant ENaC activity in the apical membrane of *Scnn1a*^{loxloxCre} mice. We assessed the response to amiloride by the criterion of a rapid decrease in inward conductance and in the current at a holding potential (V) of 0 mV or –100 mV. In cells from *Scnn1a*^{loxlox} mice, 100% of the cells tested expressed a highly significant amiloride-sensitive current at V = 0 mV (141 ± 22 pA per cell), whereas none of the cells from *Scnn1a*^{loxloxCre} mice had a current significantly different from 0 (–5 ± 2 pA per cell). The difference between the two groups was significant ($P < 0.001$) (Table 2, bottom). We measured the amiloride-sensitive current at V = –100 mV, which would greatly favor the entry of sodium through ENaC; the amiloride-sensitive current increased, as expected, over fourfold (628 ± 85 pA per cell) in cells from *Scnn1a*^{loxlox} mice, but there still was no detectable amiloride-sensitive current in cells from *Scnn1a*^{loxloxCre} mice (0.2 ± 6 pA per cell). The difference between the two groups was significant ($P < 0.001$).

Gene inactivation of ENaC in CD does not lead to a PHA-1 phenotype. On a regular diet, the *Scnn1a*^{loxloxCre} mice survived well and grew normally. There was no evidence for a salt-losing syndrome, suggesting that the expression of ENaC in the DCT and CNT was sufficient for

Table 1
Plasma aldosterone before and after sodium restriction

Plasma aldosterone (nM)			
	Control	Experimental	Control vs. experimental
	Scnn1a^{loxlox}	*Scnn1a*^{loxloxCre}	
Day 0	1.3 ± 0.26 (5)	0.9 ± 0.08 (5)	$P < 0.11$
Day 5	9.2 ± 2.7 (4)	11.7 ± 3.3 (6)	$P < 0.6$
Day 0 vs. day 5	$P < 0.02$	$P < 0.01$	

Values are means ± SEM; the numbers of mice are indicated in parentheses. Plasma aldosterone levels were measured as described in Methods. Day 0, before salt restriction; day 5, after 5 days of a sodium-deficient diet.

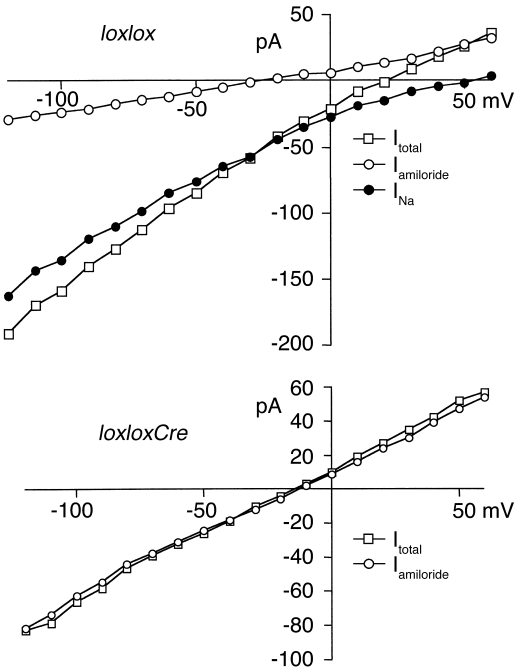

Figure 8
IV curves. Cells from isolated CCDs (protocol A) were voltage clamped to a holding potential of zero. The voltage was stepped from –120 to +60 mV in 10-mV steps, and whole-cell currents were measured at the end of each 50-millisecond pulse. The procedure was repeated after addition of 10 μM amiloride to the bath (open squares [I_{total} = total current]; open circles, current with amiloride [$I_{amiloride}$ = amiloride-resistant current]; filled circles, difference [$I_{Na} = I_{total} - I_{amiloride}$ = amiloride-sensitive current]). In cells from control (*Scnn1a*^{loxlox}) animals, a substantial fraction of the whole-cell conductance was inhibited and the amiloride-sensitive currents reversed at positive cell potentials. In cells from experimental (*Scnn1a*^{loxloxCre}) animals, no amiloride-sensitive conductance could be measured. I, electrical current expressed in picoamperes.

keeping the animals in sodium balance. We tested their ability to stand the stress of a 1-week sodium-deficient diet. This treatment was previously shown to be lethal in a mouse model with a hypomorphic β allele (βENaC$^{m/m}$), in which the βENaC mRNA level was decreased to 1% of wild type (31). With normal salt intake (0.3%), these mice showed a normal growth rate and the phenotype was clinically silent (normal plasma and urinary potassium concentrations). On a sodium-deficient (0.01%) diet, βENaC$^{m/m}$ mice developed an acute PHA-1 phenotype with rapid weight loss, which was significantly greater than that of littermate controls, by 48 hours after salt restriction. Upon a similar challenge, the *Scnn1a*^{loxloxCre} mice did not show any evidence for a salt-losing syndrome. As shown in Figure 9, they lost approximately 9% of their body weight but then were able to maintain this weight as well as their control littermates.

Gene inactivation of ENaC in CDs does not impair potassium or water balance. We then tested whether these animals could tolerate water deprivation. As shown in Figure 10, on a sodium-deficient diet, both control and test animals decreased their plasma osmolality from around 305 mOsm/l to 300 mOsm/l (Figure 10a). Urinary osmolality went down from 2,000 mOsm/l to less than 1,000 mOsm/l (Figure 10b). Upon a challenge of water deprivation for 23 hours, both strains responded quite well by raising the urinary osmolality to more than 3,000 mOsm/l, approaching the maximal urinary osmolyte concentration that can be reached in this species (32). Plasma sodium levels (Figure 10c) did not change on a sodium-deficient diet but increased significantly after 23 hours of water deprivation (Figure 10c), whereas urinary sodium decreased to less than 2 mM (Figure 10d), but there were no differences between *Scnn1a*^{loxloxCre} mice and their littermate controls. Plasma and urinary potassium remained unchanged throughout the experiments (Figure 10, e and f).

Since potassium secretion in CDs is coupled electrochemically to the electrogenic reabsorption of sodium (33), we tested the ability of the mutant mice to eliminate a potassium load. Potassium diet was raised from 0.95% (standard diet) to 2.6% for 2 days and then to 6% for 2 additional days. Plasma sodium and plasma potassium increased significantly with respect to day 0, but there was no difference between *Scnn1a*^{loxloxCre} mice and their control littermates (Figure 11, a and b). Urinary sodium and potassium increased threefold during the same period, but again there was no difference between *Scnn1a*^{loxloxCre} mice and their littermate controls (Figure 11, c and d).

Discussion

CD-specific gene inactivation of αENaC. We present evidence for the specific gene inactivation of αENaC in the CD of the mouse kidney. To our knowledge, this is the first report of inactivation of a gene normally expressed and regulated in the CD of adult mice. Tissue-specific knockouts are especially useful when the conventional knockouts lead to an early lethal phenotype and/or when the phenotype affects multiple tissues, preventing the detailed study of its function

Table 2
Effect of low-sodium diet and aldosterone infusion on sodium channels

Low sodium	Control	Experimental
(Protocol A)	*Scnn1a*^{loxlox}	*Scnn1a*^{loxloxCre}
I_{Na} (pA per cell)		
V = –100mV	102 ± 25 (12)	0^{A} (21)
Aldosterone infusion	Control	Experimental
(Protocol C)	*Scnn1a*^{loxlox}	*Scnn1a*^{loxloxCre}
I_{Na} (pA per cell)		
V = 0 mV	141 ± 22 (23)	–5 ± 2^{A} (17)
V = –100mV	628 ± 85 (23)	0.2 ± 6^{A} (17)

Values are means ± SE; the numbers of cells are indicated in parentheses. I_{Na}, amiloride-sensitive currents. $^{A}P < 0.001$ (significantly different from control values). V, voltage.

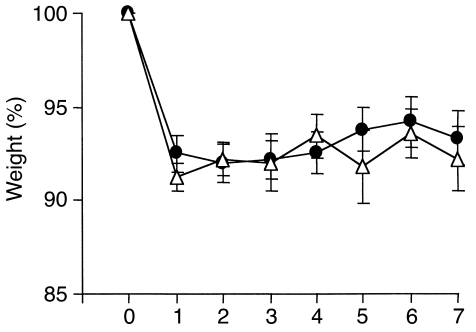

Figure 9
Body-weight loss under salt restriction. Body-weight measurements in adult *Scnn1a*^{loxlox} (n = 9, filled circles) and *Scnn1a*^{loxloxCre} (n = 9, open triangles) mice. Animals were kept on a normal-salt diet (0.23% sodium) until day 0, followed by a sodium-deficient diet (0% sodium) for 7 days. Body weights of each group are indicated as percentages of the reference weight (100% at day 0). Mice were weighed at the same time each day.

in a particular lineage (34, 35). The number of successful conditional knockout experiments reported in the literature is rapidly growing (34), but there are still few reports concerning the use of *Cre* mice expressing a kidney-specific promoter. Nelson et al. (36) reported that a 14-kb aquaporin promoter conferred cell-specific expression in the renal CD, in the epithelial cells of the vas deferens, and within the testis. To our knowledge, this transgenic mouse has not shown complete inactivation of a functional gene normally expressed in this nephron segment. Shao et al. (37) recently reported the use of a cadherin promoter, a member of the cadherin family expressed in tubular epithelial cells in the kidney and in developing genitourinary tracts. In adult mice, the expression was restricted to the CD and the thick ascending limb of Henle's loop. This model should be useful for kidney-specific gene targeting, although the efficiency of *Cre/lox* recombination in the CD could not be determined with accuracy.

In the present study, we have no evidence for cell-autonomous expression or significant mosaicism. The specificity of recombination is high because *Hoxb7* is expressed early in development and limited to the CD for the galactosidase reporter gene (Figure 1). The efficiency of recombination is also high because immunodetection of α, β, and γ subunits colocalized (under salt restriction) at the apical membrane of the principal cells of the CD is a sensitive assay. Hundreds of cells can be screened on kidney sections, and we found that the recombination event from αENaC was close to 100%, since less than 1.5% αENaC-positive cells were observed. Furthermore, measurement of ENaC at the single-cell level by patch clamp can detect cells with amiloride-sensitive current with fairly good accuracy. The total number of cells screened was, for technical reasons, more limited that for immunofluorescent screening. Nevertheless, no cells from *Scnn1a*^{loxloxCre} ever expressed an amiloride-sensitive current. The observed deletion of αENaC expression extends along the entire CCD and OMCD. We cannot say whether the αENaC gene is also inactivated in IMCD, because under the present protocol of 6 days of salt restriction, we were not able to detect any expression of ENaC α, β or γ subunits in this part of the CD of control animals. Gene inactivation of αENaC in OMCD and CCD is highly specific, since β and γENaC genes as well as AQP2 and CB are expressed normally. The reason for such selectivity is not known, but the fact that *Hoxb7* is mainly expressed in the late phase of metanephros development, specifically during ureteric bud branching morphogenesis, may be one of the reasons for the results reported here (21, 27).

In vivo evidence for preferential assembly of ENaC subunits in ASDN. In vitro in the *Xenopus* oocyte expression system, the α subunit plays an essential role in the trafficking of the channel to the cell surface (5). Maximal ENaC activity is observed only upon coinjection of αβγ cRNA subunits to form a heterotetramer (α2βγ) (8, 9). α2β2 and α2γ2 heterodimers lead to 10–15% of the maximal activity, whereas β2γ2 leads to a very small although significant activity (1–2% of maximal activity). It is not clear whether such β2γ2 channels can be exported to the apical membrane of the principal cell in vivo. In the present experiment, αENaC expression is totally suppressed along the CD, and we could not detect any significant amount of β or γ subunits in subapical or apical membranes of the principal cell, despite the presence of a strong stimulus (high plasma aldosterone) (Figure 9) to relocalize ENaC at the apical membrane (13), as clearly seen in the control littermates. ENaC activity, as measured by patch-clamp experiments, was also undetectable in the principal cells of CCDs, whereas it was readily measured in the control littermates. As discussed recently (38), we cannot, however, completely rule out the possibility that a small yet undetectable pool of ENaC channels made of β2γ2 subunits could be present in the apical membrane and contribute to some constitutive sodium reabsorption in this part of the nephron. Such a small pool is expected to ensure survival in the presence of a normal-salt diet but should not be sufficient to keep the body in sodium balance when challenged by a sodium-deficient (close to zero salt) diet, as shown in two models of PHA-1. In a previously described mouse model for PHA-1 (39), the transgenic expression of αENaC was driven by the aldosterone-independent cytomegalovirus promoter onto an αENaC knockout (αENaC$^{-/-}$ Tg) genetic background. Young mice developed a renal salt wasting syndrome, and 50% died within 2 weeks after birth. Adult αENaC$^{-/-}$ Tg survivors exhibited a compensated PHA-1 phenotype, with a constitutive but diminished expression (measured at the mRNA level) of the α transgene in lung and kidney.

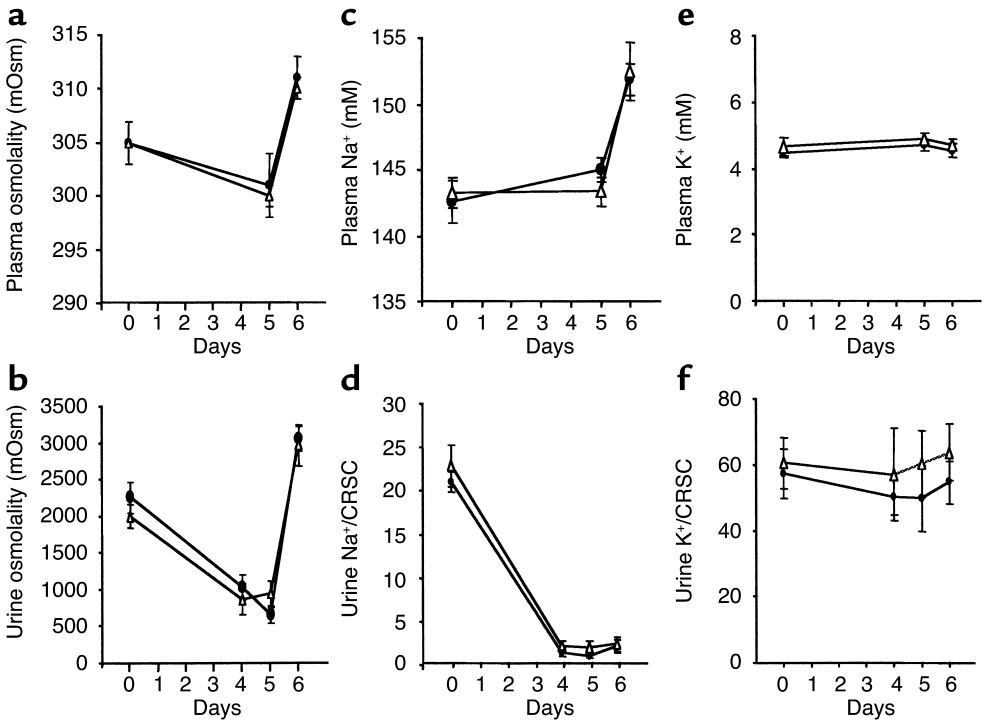

Figure 10
Salt and water restriction. Urine and plasma osmolalities and physiological measurements in adult *Scnn1a*^{loxlox} (n = 9, filled circles) and *Scnn1a*^{loxloxCre} (n = 9, open triangles) mice. Animals were kept on a normal-salt diet (0.23% sodium) until day 0, followed by a sodium-deficient diet (0% sodium) for 5 days with free access to water. Osmolalities were measured at day 0 during the normal-salt diet and during a sodium-deficient diet before and after 23 hours of water deprivation (each group, n = 8).(**a**) Plasma osmolality in mice of indicated genotype. (**b**) Urine osmolality in mice of indicated genotype. Physiological measurements were performed at day 0 during the normal-salt diet and after 5 days of a sodium-deficient diet before and after 23 hours of water deprivation (each group, n = 8). (**c**) Plasma sodium levels. (**d**) Relative values of urine sodium normalized with creatinine. (**e**) Plasma potassium levels. (**f**) Relative values of urine potassium normalized with creatinine. CRSC, creatinine measured by single-slide method.

In a second mouse model, salt restriction could induce PHA-1 in mice having a hypomorphic β subunit ENaC allele ($\beta^{m/m}$) (31). Interestingly, these mice showed a low level of βENaC mRNA expression in the kidney (1% of wild type). In homozygous mutant $\beta ENaC^{m/m}$ mice, no βENaC protein could be detected using immunohistochemistry in lung or kidney. The phenotype was clinically silent on a normal-salt diet, but mice developed acute PHA, weight loss, hyperkalemia, and decreased blood pressure within 2 days of salt deprivation. In this model, where αγENaC expression is maintained, it was expected that two kinds of channels — α2γ2 or $\alpha 2\beta_m\gamma$ — could be formed, which altogether could ensure a significant ENaC activity along the entire ASDN. Of course, these two mouse models did not address the question raised in the present paper — what was the *relative* contribution of ENaC expression in late DCT/CNT versus CD — but they indicate that survival may depend on a small pool of ENaC proteins (not detectable by

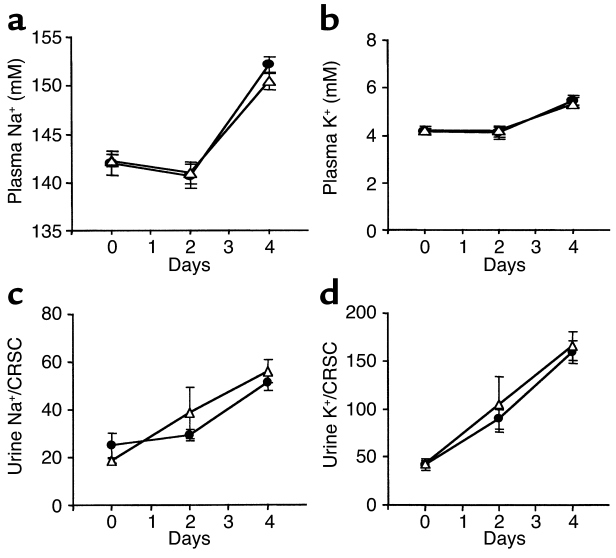

Figure 11
Physiological measurements under potassium loading in adult *Scnn1a*^{loxlox} (n = 9, filled circles) and *Scnn1a*^{loxloxCre} (n = 9, open triangles) mice. Animals were kept on a normal diet (0.95% potassium) until day 0 and then were fed a diet containing 2.6% potassium for 2 days followed by a diet containing 6% potassium for 2 days (each group, n = 6). (**a**) Plasma sodium levels. (**b**) Plasma potassium levels. (**c**) Relative values of urine sodium normalized with creatinine. (**d**) Relative values of urine potassium normalized with creatinine.

immunostaining) along the entire ASDN. However, when the normal regulation is lost, the animal cannot survive salt restriction. By deleting αENaC specifically in CDs, we expected a phenotype similar to that described in our two models of PHA-1.

Role of late DCT and CNT: the sodium transport capacity of these segments far exceeds that of CCD and/or OMCD. The present paper shows that, despite undetectable ENaC activity in CCD principal cells, the animals stay in sodium and potassium balance. The conclusion that the CD may play a minor role in sodium conservation under conditions of salt restriction is perhaps not that surprising. In their classic micropuncture observations in the rat, Malnic et al. (40) found that, even with normal dietary sodium intake, 8–10% of the filtered load of sodium reached the early DCT but less than 1% was present in the late DCT. It should be noted that the results were obtained using free-flow micropuncture of the DCT. Thus, the late DCT sampled in these studies should probably be more proximal to the CNT discussed in the present paper. These studies demonstrated that even under normal dietary conditions, the DCT and CNT reabsorb more than 90% of the sodium that is delivered to ASDN.

The CDs are formed in the renal cortex by the joining of several nephrons (41). The location of the exact border between the nephron and a CD is not yet clear. The CNT is interposed between the nephron and the CCD (41). The embryonic origin of CNT is controversial, but in the present experiments, it is clear that the *Hoxb7* promoter stops its expression at a sharp border between the CNT and the CCD. A CNT from a superficial nephron normally joins one CCD, whereas CNTs from deep nephrons join to form an arcade before draining into a CCD. The length of a CNT arcade can be as long as 1 mm. The distribution of apically located sodium and water transport proteins in the distal nephron of rabbits, rats, mice, and human (42) has been recently reported, allowing anatomophysiological correlations. In mice, the early portion of DCT expresses the sodium thiazide–sensitive chloride cotransporter (NCC). In the more distal part of the DCT (late DCT), there is overlapping expression between NCC and ENaC, whereas CNT is characterized by the lack of NCC expression and the expression of ENaC and AQP2. The morphology of late DCT cells, CNT cells, and CCD principal cells differs markedly (41). The most striking is the progressive decrease, from late DCT to CCD, of the basolateral membrane infoldings and the mitochondrial density, suggesting different metabolic rates. Corresponding to these anatomical features, the rate of sodium transport appears to be quite different between the CNT and the CCD. Measurement of sodium fluxes in isolated rabbit CNTs (43, 44) or from rabbit CCDs (45) or rat CCDs (46) indicates at least a 10-fold difference (120–600 pmol versus 0.2–24 pmol of sodium per minute per millimeter in CCD). The rates of sodium transport in OMCD and IMCD are generally low (47) but have been measured only in rabbits (8 versus 1 pmol per minute per millimeter, respectively). CNT cells are also fully equipped with proteins necessary for responding to aldosterone (mineralocorticoid receptor, 11-β-HSD2, sgk-1, ENaC, and Na,K-ATPase). The CNT cell is also able to secrete potassium (48, 49), and potassium loading induces morphogenetic changes in this cell (49, 50). ROMK is expressed in the apical membrane of DCT and CNT cells (51, 52). Our data stress and reemphasize the specific role of the CNT cell in the ASDN to achieve sodium and potassium balance, even under stressful conditions such as salt restriction and/or salt and water restriction. Data on the function of CNT remain limited, mainly because of technical difficulties in isolating this segment and the impossibility so far to measure ENaC activity by patch clamp, a measurement already performed on CCD more than 15 years ago (53).

Role of ENaC expression in CCD. The results presented here indicate that channel-mediated transport in the late DCT/CNT, with apparently no contribution from the CCD, is sufficient to maintain sodium and potassium balance. The role of the well-studied sodium and potassium transport systems in the CCD in electrolyte homeostasis comes into question. However, there is abundant evidence that ENaC in the CCD is regulated by aldosterone in response to both short-term and long-term sodium restriction. The main difference between the responses in DCT2/CNT versus CCD may therefore be *quantitative* rather than qualitative, with a large proportion of the aldosterone-regulated transport occurring before the tubular fluid reaches the collecting duct. The late DCT/CNT cells could then be further upregulated to compensate for the loss of transport by the CCD. Frindt et al. (22) have recently reported that pharmacological inactivation of ENaC, by chronic administration of the ENaC blocker amiloride, resulted in a salt-losing syndrome similar to that observed in mice carrying the hypomorphic ENaC β allele discussed above and certainly more severe than that described in the present study. Comparison of these results strongly suggests that the maintained ability to control sodium balance in the absence of ENaC in CCD depends on ENaC expression in other nephron segments rather than on other (amiloride-insensitive) transport pathways in the CD.

Acknowledgments

We thank Jean-Daniel Horisberger for critically reading the manuscript, Nicole Skarda for secretarial work, and Hans-Peter Gaeggeler for photographic work. This work was supported by grants from the Swiss National Foundation (32-061742.00 to J. Loffing, 31-063801.00 to E. Hummler, and 31-061966.00 to B.C. Rossier) and by NIH grant DKDK59659 to L.G. Palmer.

1. Verrey, F., Hummler, E., Schild, L., and Rossier, B.C. 2000. Control of Na^+ transport by aldosterone. In *The kidney: physiology and pathophysiology*. Volume 1. Third edition. D.W. Seldin and G. Giebisch, eds. Lippincott, Williams, and Wilkins. Philadelphia, Pennsylvania, USA. 1441–1471.
2. Canessa, C.M., et al. 1994. The amiloride-sensitive epithelial sodium channel is made of three homologous subunits. *Nature.* **367**:463–467.
3. Firsov, D., et al. 1996. Cell surface expression of the epithelial Na channel and a mutant causing Liddle syndrome: a quantitative approach. *Proc. Natl. Acad. Sci. U. S. A.* **93**:15370–15375.
4. Firsov, D., Gautschi, I., Merillat, A.M., Rossier, B.C., and Schild, L. 1998. The heterotetrameric architecture of the epithelial sodium channel (ENaC). *EMBO J.* **17**:344–352.
5. Bonny, O., et al. 1999. Functional expression of a pseudohypoaldosteronism type I mutated epithelial Na^+ channel lacking the pore-forming region of its α subunit. *J. Clin. Invest.* **104**:967–974.
6. Rossier, B.C., Pradervand, S., Schild, L., and Hummler, E. 2002. Epithelial sodium channel and the control of sodium balance: interaction between genetic and environmental factors. *Annu. Rev. Physiol.* **64**:877–897.
7. Shimkets, R.A., et al. 1994. Liddle's syndrome: heritable human hypertension caused by mutations in the β subunit of the epithelial sodium channel. *Cell.* **79**:407–414.
8. Chang, S.S., et al. 1996. Mutations in subunits of the epithelial sodium channel cause salt wasting with hyperkalaemic acidosis, pseudohypoaldosteronism type 1. *Nat. Genet.* **12**:248–253.
9. Loffing, J., et al. 2001. Aldosterone induces rapid apical translocation of ENaC in early portion of renal collecting system: possible role of SGK. *Am. J. Physiol.* **280**:F675–F682.
10. Pacha, J., Frindt, G., Antonian, L., Silver, R.B., and Palmer, L.G. 1993. Regulation of Na channels of the rat cortical collecting tubule by aldosterone. *J. Gen. Physiol.* **102**:25–42.
11. Duc, C., Farman, N., Canessa, C.M., Bonvalet, J.P., and Rossier, B.C. 1994. Cell-specific expression of epithelial sodium channel α, β, and γ subunits in aldosterone-responsive epithelia from the rat: localization by in situ hybridization and immunocytochemistry. *J. Cell Biol.* **127**:1907–1921.
12. Masilamani, S., Kim, G.H., Mitchell, C., Wade, J.B., and Knepper, M.A. 1999. Aldosterone-mediated regulation of ENaC α, β, and γ subunit proteins in rat kidney. *J. Clin. Invest.* **104**:R19–R23.
13. Loffing, J., et al. 2000. Differential subcellular localization of ENaC subunits in mouse kidney in response to high- and low-Na diets. *Am. J. Physiol.* **279**:F252–F258.
14. Horisberger, J.-D., and Diezi, J. 1983. Effects of mineralocorticoids on Na^+ and K^+ excretion in the adrenalectomized rat. *Am. J. Physiol.* **245**:F89–F99.
15. Hummler, E., et al. 1996. Early death due to defective neonatal lung liquid clearance in α-ENaC-deficient mice. *Nat. Genet.* **12**:325–328.
16. Barker, P.M., et al. 1998. Role of γ ENaC subunit in lung liquid clearance and electrolyte balance in newborn mice. *J. Clin. Invest.* **102**:1634–1640.
17. McDonald, F.J., et al. 1999. Disruption of the β subunit of the epithelial Na+ channel in mice: Hyperkalemia and neonatal death associated with a pseudohypoaldosteronism phenotype. *Proc. Natl. Acad. Sci. U. S. A.* **96**:1727–1731.
18. Hummler, E., Merillat, A.M., Rubera, I., Rossier, B.C., and Beermann, F. 2002. Conditional gene targeting of the Scnn1a (αENaC) gene locus. *Genesis.* **32**:169–172.
19. Meisler, M.H., Barrow, L.L., Canessa, C.M., and Rossier, B.C. 1994. SCNN1, an epithelial cell sodium channel gene in the conserved linkage group on mouse chromosome 6 and human chromosome 12. *Genomics.* **24**:185–186.
20. Pathak, B.G., et al. 1996. Mouse chromosomal location of three epithelial sodium channel subunit genes and an apical sodium chloride cotransporter gene. *Genomics.* **33**:124–127.
21. Yu, J., Carroll, T.J., and McMahon, A.P. 2002. Sonic hedgehog regulates proliferation and differentiation of mesenchymal cells in the mouse metanephric kidney. *Development.* **129**:5301–5312.
22. Frindt, G., McNair, T., Dahlmann, A., Jacobs-Palmer, E., and Palmer, L.G. 2002. Epithelial Na channels and short-term renal response to salt deprivation. *Am. J. Physiol.* **283**:F717–F726.
23. Kress, C., et al. 1990. Hox-2.3 upstream sequences mediate lacZ expression in intermediate mesoderm derivatives of transgenic mice. *Development.* **109**:775–786.
24. de Graaff, E., et al. 2001. Differential activities of the RET tyrosine kinase receptor isoforms during mammalian embryogenesis. *Genes Dev.* **15**:2433–2444.
25. Srinivas, S., et al. 1999. Expression of green fluorescent protein in the ureteric bud of transgenic mice: a new tool for the analysis of ureteric bud morphogenesis. *Dev. Genet.* **24**:241–251.
26. Srinivas, S., Wu, Z., Chen, C.M., D'Agati, V., and Costantini, F. 1999. Dominant effects of RET receptor misexpression and ligand-independent RET signaling on ureteric bud development. *Development.* **126**:1375–1386.
27. Rauchman, M. 2000. The role of homeobox genes in kidney development. *Curr. Opin. Nephrol. Hypertens.* **9**:37–42.
28. Srivinas, S., et al. 2001. Cre reporter strains produced by targeted insertion of EYFP and ECFP into the RPSA26 locus. *BMC Dev. Biol.* **208**:281–292.
29. Frindt, G., Masilamani, S., Knepper, M.A., and Palmer, L.G. 2001. Activation of epithelial Na channels during short-term Na deprivation. *Am. J. Physiol.* **280**:F112–F118.
30. Schafer, J.A., and Chen, L. 1998. Low Na^+ diet inhibits Na^+ and water transport response to vasopressin in rat cortical collecting duct. *Kidney Int.* **54**:180–187.
31. Pradervand, S., et al. 1999. Salt restriction induces pseudohypoaldosteronism type 1 in mice expressing low levels of the β-subunit of the amiloride-sensitive epithelial sodium channel. *Proc. Natl. Acad. Sci. U. S. A.* **96**:1732–1737.
32. Yang, B., Gillespie, A., Carlson, E.J., Epstein, C.J., and Verkman, A.S. 2001. Neonatal mortality in an aquaporin-2 knock-in mouse model of recessive nephrogenic diabetes insipidus. *J. Biol. Chem.* **276**:2775–2779.
33. Giebisch, G. 1998. Renal potassium transport: mechanisms and regulation. *Am. J. Physiol.* **43**:F817–F833.
34. Kwan, K.-M. 2002. Conditional alleles in mice: practical considerations for tissue-specific knockouts. *Genesis.* **32**:49–62.
35. Jaisser, F. 2000. Inducible gene expression and gene modification in transgenic mice. *J. Am. Soc. Nephrol.* **11**:S95–S100.
36. Nelson, R.D., et al. 1998. Expression of an AQP2 Cre recombinase transgene in kidney and male reproductive system of transgenic mice. *Am. J. Physiol.* **275**:C216–C226.
37. Shao, X., Somlo, S., and Igarashi, P. 2002. Epithelial-specific Cre/lox recombination in the developing kidney and genitourinary tract. *J. Am. Soc. Nephrol.* **13**:1837–1846.
38. Rossier, B.C. 2002. Hormonal regulation of the epithelial sodium channel ENaC: N or Po? *J. Gen. Physiol.* **120**:67–70.
39. Hummler, E., et al. 1997. A mouse model for the renal salt-wasting syndrome pseudohypoaldosteronism. *Proc. Natl. Acad. Sci. U. S. A.* **94**:11710–11715.
40. Malnic, G., Klose, R.M., and Giebisch, D.W. 1964. Micropuncture study of renal potassium excretion in the rat. *Am. J. Physiol.* **206**:674–686.
41. Kriz, R.W., and Kaissling, B. 2000. Structural organization of the mammalian kidney. In *The kidney: physiology and pathophysiology*. Volume 1. Third edition. D.W. Seldin and G. Giebisch, eds. Lippincott, Williams, and Wilkins. Philadelphia, Pennsylvania, USA. 587–654.
42. Biner, H.L., et al. 2002. Human cortical distal nephron: distribution of electrolyte and water transport pathways. *J. Am. Soc. Nephrol.* **13**:836–847.
43. Almeida, A.J., and Burg, M.B. 1982. Sodium transport in the rabbit connecting tubule. *Am. J. Physiol.* **243**:F330–F334.
44. Shareghi, G.R., and Stoner, L.C. 1978. Calcium transport across segments of the rabbit distal nephron in vitro. *Am. J. Physiol.* **235**:F367–F375.
45. Tomita, K., Pisano, J.J., and Knepper, M.A. 1985. Control of sodium and potassium transport in the cortical collecting duct of the rat. Effects of bradykinin, vasopressin, and deoxycorticosterone. *J. Clin. Invest.* **76**:132–136.
46. Reif, M.C., Troutman, S.L., and Schafer, J.A. 1968. Sodium transport by rat cortical collecting tubule: effects of vasopressin and desoxycorticosterone. *J. Clin. Invest.* **77**:1291–1298.
47. Stokes, J.B. 1982. Ion transport by the cortical and outer medullary collecting tubule. *Kidney Int.* **22**:473–484.
48. Malnic, G., Muto, S., and Giebisch, G. 2000. Regulation of potassium excretion. In *The kidney: physiology and pathophysiology*. Volume 1. Third edition. D.W. Seldin and G. Giebisch, eds. Lippincott, Williams, and Wilkins. Philadelphia, Pennsylvania, USA. 1575–1613.
49. Stanton, B.A., and Giebisch, G. 1981. Mechanism of urinary potassium excretion. *Miner. Electrolyte Metab.* **5**:100–120.
50. Kaissling, B., and Le Hir, M. 1982. Distal tubular segments of the rabbit kidney after adaptation to altered Na- and K-intake. *Cell Tissue Res.* **224**:469–492.
51. Xu, J.Z., et al. 1997. Localization of the ROMK protein on apical membranes of rat kidney nephron segments. *Am. J. Physiol.* **273**:F739–F748.
52. Mennitt, P.A., Wade, J.B., Ecelbarger, C.A., Palmer, L.G., and Frindt, G. 1997. Localization of ROMK channels in the rat kidney. *J. Am. Soc. Nephrol.* **8**:1823–1830.
53. Palmer, L.G., and Frindt, G. 1986. Amiloride-sensitive Na channels from the apical membrane of the rat cortical collecting tubule. *Proc. Natl. Acad. Sci. U. S. A.* **83**:2767–2770.